

# Three-dimensional particle imaging by defocusing method with an annular aperture

Dejiao Lin,<sup>1</sup> Natalia C. Angarita-Jaimes,<sup>1</sup> Siyu Chen,<sup>1</sup> Alan H. Greenaway,<sup>2</sup> Catherine E. Towers,<sup>1</sup> and David P. Towers<sup>1,\*</sup>

<sup>1</sup>*School of Mechanical Engineering, University of Leeds, Leeds LS2 9JT, UK*

<sup>2</sup>*School of Engineering and Physical Science, Heriot-Watt University, Edinburgh EH14 4AS, UK*

\*Corresponding author: *d.p.towers@leeds.ac.uk*

Received December 17, 2007; revised March 7, 2008; accepted March 14, 2008;  
posted March 20, 2008 (Doc. ID 89837); published April 22, 2008

We propose an annular-aperture-based defocusing technique for three-dimensional (3D) particle metrology from a single camera view. This simple configuration has high optical efficiency and the ability to deal with overlapped defocused images. Initial results show that an uncertainty in depth of  $23\ \mu\text{m}$  can be achieved over a range of 10 mm for macroscopic systems. This method can also be applied in microscopy for the measurement of fluorescently doped microparticles, thus providing a promising solution for 3D flow metrology at both macroscales and microscales. © 2008 Optical Society of America  
OCIS codes: 120.7250, 120.3940, 110.1220, 110.6880, 180.0180.

The measurement of three components (3C) of fluid velocity within a three-dimensional (3D) flow volume is essential to further the understanding of turbulent flow structures and for the validation of computational fluid dynamics predictions. Three-components three-dimensional (3C3D) flow measurement via particle image velocimetry (PIV) has evoked much interest in recent years [1–9].

Stereo PIV is widely used but provides only 3C velocity data over a two-dimensional (2D) plane [3]. Holographic PIV offers 3C3D velocity measurement [4] and can produce high-resolution data over a volume but requires wet processing and time-consuming hologram interrogation. Moreover, holographic-based methods cannot be applied to the self-luminous tracers typically required in microfluidics. More recently, tomographic PIV looks promising for 3D flow measurement; nonetheless it requires excellent optical access for, typically, four cameras and computationally expensive data processing [5]. From a basis in machine vision [6], defocusing digital PIV (DDPIV) uses multiple small apertures to produce the same number of images of each particle and to encode information about depth location [7,8]. An off-axis rotating pinhole aperture was used to effect a spacing between images of out-of-focus objects so as to determine the 3D position of the object [9]. However, the small apertures used make these techniques optically inefficient and restrict the applications to those where brighter, typically larger, tracer particles can be used. Wavefront sensing has recently been applied to 3C3D particle velocimetry [2,10] but, despite being optically efficient and compatible with coherent and incoherent sources, can only be used with flows where the seed density is kept relatively low.

In this Letter we propose a novel defocusing technique using an annular aperture to obtain 3C3D measurements. Annular apertures have been widely explored for increasing focal depth in optical systems so as to enhance image quality [11,12]. The approach offers a simple optical configuration and by locating the clear annulus toward the outer edge of the imaging lens the optical efficiency is maximized and is

$>5\times$  the total aperture area used in DDPIV. With respect to existing wavefront sensing techniques for 3C3D measurement [10] this technique can resolve overlapped particle images, which appear as interlocking rings and thereby offer increased spatial resolution for 3D velocity measurements in fluid flows. Moreover, the technique can also be applied in microscopy. We present the imaging setup and data processing methodology with initial results from both macroscopic and microscopic configurations.

Figure 1 illustrates a schematic of the 3D particle metrology approach, where an annular aperture is placed close to an idealized converging lens. A ring-shaped image is observed on the CCD camera when the tracer is out of focus. From the size of the defocused image, a function of the outer and inner diameters of the annular aperture, the particle's  $z$  coordinate can be determined. Combined with the  $x$ – $y$  positions, obtained from the image center of mass, the 3D position of the tracer can be reconstructed from a single view.

As shown in Fig. 1 for a geometric optics model, the image of a particle at position  $P_0(x_0, y_0, z_0)$  is focused on the image plane at  $P'_0$ , thereby  $z=z_0=0$  corresponds to the in-focus plane. As the particle's position moves away from this plane, the resulting out-of-focus image becomes ring-shaped and the particle at position  $P_1(x_1, y_1, z_1)$  generates an annular image

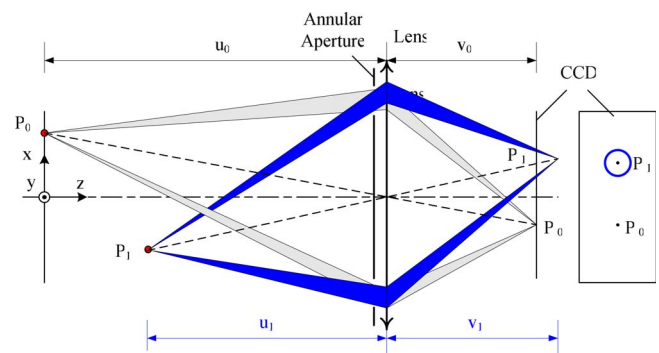


Fig. 1. (Color online) Schematic of optical setup for 3D PIV using annular aperture.

with the center at  $P_1'$ . Suppose the outer and inner diameters of the annular aperture are  $D_{\text{out}}$  and  $D_{\text{in}}$ , respectively, then the average diameter of the annular image,  $D_{\text{im}}$ , is given by

$$D_{\text{im}} = \frac{(u_0 - u_1)f}{(u_0 - f)u_1} D_{\text{av}}, \quad (1)$$

where  $D_{\text{av}} = (D_{\text{out}} + D_{\text{in}})/2$ ,  $f$  is the focal length of the lens, and  $u_0$  and  $u_1$  are the object distances of  $P_0$  and  $P_1$ . There are two special cases from Eq. (1):  $D_{\text{im}} = 0$  when  $u_1 = u_0$  and  $D_{\text{im}} = D_{\text{av}}$  when  $u_1 = f$ . From Eq. (1), the measurement sensitivity, or rate of change of  $D_{\text{im}}$  with respect to  $u_1$ , is

$$\frac{d(D_{\text{im}})}{d(u_1)} = -D_{\text{av}} \frac{u_0 f}{(u_0 - f)u_1^2}. \quad (2)$$

Equations (1) and (2) are valid only when the particle is some distance from the in-focus plane. Diffraction effects should be considered when the particle is near the focal plane, in which case the rigorous expression using Lommel functions should be used when  $u_0 \approx u_1$  [11].

To estimate the inner and outer diameters and therefore the out-of-plane position, it is necessary to perform some processing on the annular images. To reduce the effects of noise and diffraction, the average radial profile is taken for each annular image [see Figs. 2(a) and 2(b)]. Once the maximum peaks at each side are identified, two one-dimensional (1D) intensity profiles are generated; see Fig. 2(b). Rotating these projections about the image center of mass, a pair of 2D images are obtained from which the diameters can be calculated using a threshold [10] or the images can be used as wavefront sensor input. The

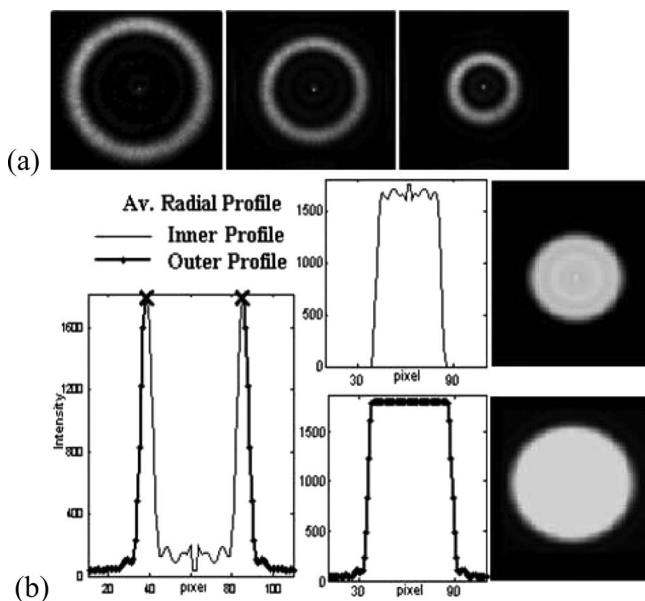


Fig. 2. Annular images and processing: (a) images at different depth positions, (b) average radial profile with the inner and outer diameters of the annulus separated by local maxima. From the inner and outer profiles, two spherical images are reconstructed and the diameters of these are calculated.

Seidel defocus is extracted from the outer and inner diameters. To evaluate sensor performance a least-squares fit has been carried out between the known depth positions of a test source and the Seidel defocus values. When  $P_0$  is outside the flow volume no depth ambiguity exists. If the in-focus plane is within the flow volume, the out-of-plane particle position can be uniquely defined by placing additional coding in the annulus.

The performance of the 3D particle imaging system has been evaluated using a single-mode fiber source to simulate a tracer particle. An  $x$ - $y$ - $z$  motorized traverse was used to position the fiber within the measurement volume (bidirectional repeatability  $< 0.5 \mu\text{m}$ ; absolute accuracy  $10 \mu\text{m}$ ). In the experiments we used a 60 mm focal length achromatic lens with an annular aperture defined by  $D_{\text{out}} = 9 \text{ mm}$  and  $D_{\text{in}} = 7 \text{ mm}$ . The source intensity was set to give similar flux levels to those from micrometer-sized tracers typically used in gas phase flows. The images were recorded on a La Vision Imager CCD with  $1376 \times 1024$  pixels and 12-bit image depth.

The experiments were performed at a mean object distance of 350 mm, giving a measurement volume of  $35 \times 27 \times 35 \text{ mm}$  ( $x, y, z$ ). The  $x$ - $y$  location of the images is estimated to  $\sim 0.1$  pixel accuracy using a center of mass calculation. Preliminary results for the depth ( $z$ ) uncertainty, based on the average of the outer and inner diameters, give a resolution of  $114 \mu\text{m}$  (to one standard deviation). The resolution achieved is magnification dependent, with a mean object distance of 160 mm a resolution of  $23 \mu\text{m}$  over a depth range of 10 mm has been obtained.

An experimental system was established to test the 3D annular aperture PIV method in microscopy. A microscope was used in an epifluorescent arrangement with an annular aperture,  $D_{\text{out}} = 5 \text{ mm}$  and  $D_{\text{in}} = 3 \text{ mm}$ , bonded to the back of a  $20\times$  infinity corrected objective. A slide with fluorescently doped microparticles is applied as a sample and fixed to a piezoelectric transducer (PZT) driven stage. By combining images with the sample in different planes a composite image is generated where the particle density and depth range can be controlled; furthermore, a sequence of images can be captured representing a PIV image pair. Figure 3(a) shows a typical combined image containing  $\sim 450$  particles from a measurement volume  $\sim 410 \times 310 \times 120 \mu\text{m}$  on a detector with  $1280 \times 960$  pixels. A series of images

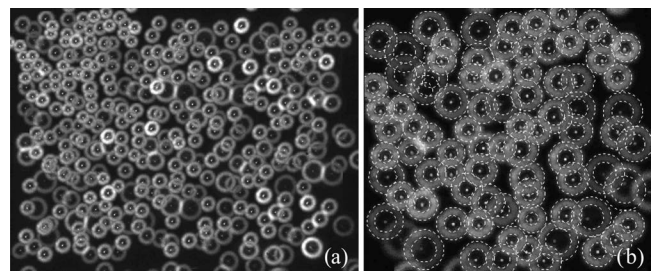


Fig. 3. (a) Combined image of multiple fluorescently doped microparticles from a microscope using an annular aperture. (b) Identification of annular images by the CHT where each edge is indicated by a broken circle.

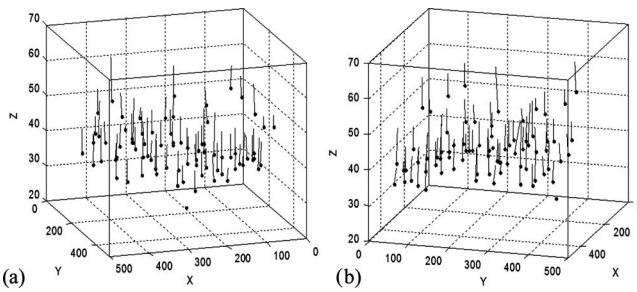


Fig. 4. (a) and (b) Two views of a 3C3D vector field reconstructed from an image pair processed via the CHT and inner-outer diameter analysis.

were recorded with the sample scanned over  $4.5 \mu\text{m}$  in steps of  $25 \text{ nm}$  (step resolution  $< 1 \text{ nm}$ ). Analyzing the annular aperture image of a single particle and based on the actual positions of the particles from the  $z$ -axis scan of the microscope an uncertainty of  $180 \text{ nm}$  was obtained. The measurement resolution can be improved dramatically when the magnification of the microscope objective is increased, and the method can be applied for live cell measurements with nanometer resolution.

One of the benefits of using an annular aperture is that the ring-shaped images facilitate the separation of overlapping particles, i.e., tracer particles with similar  $x$ - $y$  coordinates but different  $z$  coordinates, to give higher spatial resolution velocity field measurements. Initial results have been obtained using a circular Hough transform (CHT) algorithm [13]. The CHT automatically identifies circular features in the image based on intensity gradient information. The parameters estimated by the CHT, radius and center coordinates  $(x, y)$ , are used to decide which pixels in the overlapping images belong to individual rings. In this way, individual annular particle images are obtained and can be processed to extract their diameters. The algorithm is memory intensive and a  $450 \times 450$  pixel region of the image in Fig. 3(a) has been processed. The result is depicted in Fig. 3(b) where each circular feature is identified as a broken circle. It can be seen that the vast majority of the inner and outer edges of the annular aperture images have been correctly identified despite the presence of overlapping rings and the variation in defocus (size of the rings) present. A corresponding region of a second combined image was processed where each of the constituent images has a 3C displacement (all  $z$  displacements were in the same direction for clarity). Two views of the 3C3D vector field are shown in Figs. 4(a) and 4(b) with  $\sim 80$  vectors from the  $450 \times 450$  pixel region. Each axis scale is in pixels with the  $z$  axis representing pixels of defocus from the in-focus plane. This proof of principle result when scaled to current  $2048^2$  pixel CCDs implies that over 1500 3C3D vectors should be measurable using an annular

aperture from a single camera and single point of view.

We have presented a novel method that uses an annular aperture and wavefront defocus to realize 3D position measurements across a volume. It has been demonstrated that 3D resolution can be obtained from a single viewpoint with a simple configuration and high optical efficiency. The approach means that when particle images overlap, the information is present as interlocking rings that have been separated using a CHT. Hence this combined optical encoding and digital processing approach has the potential to provide high spatial resolution in densely seeded fluid flows. A depth resolution of  $23 \mu\text{m}$  has been achieved over a range of  $10 \text{ mm}$ , while in microscopy a depth resolution of  $180 \text{ nm}$  was obtained with a  $20\times$  objective. The depth resolution can be further improved using a higher magnification or a CCD camera with smaller pixel size. Further investigations are being directed on the combination of annular apertures with anamorphic optics [2], where astigmatism can uniquely resolve depth either side of focus, and the applications of these approaches to the dynamics in live cells. Such systems can be made telecentric if required [14].

The authors acknowledge funding from the Engineering and Physical Sciences Research Council (EPSRC) through grants GR/S61720 and GR/S96555 and support from La Vision.

## References

1. K. D. Hinsch, *Meas. Sci. Technol.* **6**, 742 (1995).
2. C. E. Towers, D. P. Towers, H. I. Campbell, S. Zhang, and A. H. Greenaway, *Opt. Lett.* **31**, 1220 (2006).
3. M. P. Arroyo and C. A. Greated, *Meas. Sci. Technol.* **2**, 1181 (1991).
4. D. H. Barnhart, N. A. Halliwell, and J. M. Coupland, *Proc. R. Soc. London, Ser. A* **458**, 2083 (2002).
5. G. Elsinga, F. Scarano, B. Wieneke, and B. W. van Oudheusden, *Exp. Fluids* **41**, 933 (2006).
6. M. Rioux and F. Blais, *J. Opt. Soc. Am. A* **3**, 1518 (1986).
7. C. E. Willert and M. Gharib, *Exp. Fluids* **12**, 353 (1992).
8. S. Y. Yoon and K. C. Kim, *Meas. Sci. Technol.* **17**, 2897 (2006).
9. J. Rohály, J. Lammerding, F. Frigerio, and D. P. Hart, presented at the 4th International Symposium on Particle Image Velocimetry, Gottingen, Germany, September 17–19, 2001.
10. N. C. Angarita-Jaimes, E. McGhee, M. Chennaoui, H. I. Campbell, S. Zhang, C. E. Towers, A. H. Greenaway, and D. P. Towers, *Exp. Fluids* **41**, 881 (2006).
11. E. H. Linfoot and E. Wolf, *Proc. Phys. Soc. London, Sect. B* **66**, 145 (1953).
12. W. T. Welford, *J. Opt. Soc. Am.* **50**, 749 (1960).
13. R. D. Duda and P. E. Hart, *Commun. ACM* **15**, 11 (1972).
14. S. Djidel, J. K. Gansel, H. I. Campbell, and A. H. Greenaway, *Opt. Express* **14**, 8269 (2006).